23rd IAHR International Symposium on Ice

Ann Arbor, Michigan USA, May 31 to June 3, 2016

Projection of Great Lakes seasonal ice cover using multi-variable regression models

Jia Wang[1], Xuezhi Bai[2], Zifan Yang[3], Anne Clites[1], and Haoguo Hu[4]

1. *NOAA Great Lakes Environmental Research Laboratory, Ann Arbor, Michigan jia.wang@noaa.gov*
2. *Hohai University, Nanjing, China*
3. *Department of Atmospheric, Oceanic, and Space Sciences, University of Michigan, Ann Arbor, Michigan*
4. *Cooperative Institute for Limnology and Ecosystem Research, University of Michigan, Ann Arbor, Michigan*

Abstract

In this study, temporal variability of ice cover in the Great Lakes is investigated using historical satellite measurements undated from 1973 to 2015. With high ice cover in the last two winters (2013/14 and 2014/15), the trend was significantly reduced, compared to the period 1973-2013. The decadal variability in lake ice attributed to the decreased trend. It was found that 1) Great Lakes ice cover has a linear relationship with Atlantic Multidecadal Oscillation (AMO), similar to the relationship of lake ice cover with the North Atlantic Oscillation (NAO), and 2) a weak quadratic relation with the Pacific Decadal Oscillation (PDO), similar to the relationship of lake ice cover with the Niño3.4. Based on these dynamic relationships, the original multiple variable regression models established using the indices of NAO and Niño3.4 is updated by adding both AMO and PDO, as well their competing mechanism. With the AMO and PDO added, the correlation between the model and observation increases to 0.68, compared to 0.44 using NAO and Niño3.4 only. The new model was used to project the annual maximum ice coverage using projected indices of Niño3.4, NAO, PDO, and AMO. On November 30, 2015, the AMIC of 2015/16 winter was projected to be 31%.

1. Introduction

The Laurentian Great Lakes are located in the mid-latitude area of eastern North America. The westerly jet stream is located aloft at varying latitudes in the region. The fluctuations of the westerly jet stream are controlled by the North America ridge-trough system (Bai and Wang 2012), which are influenced by large-scale atmospheric teleconnection patterns such as ENSO (El Niño Southern Oscillation) and NAO (North Atlantic Oscillation) (Wang et al. 2010; Bai et al. 2012). The fluctuation of the jet stream causes large variations in the Great Lakes region on synoptic, seasonal, and interannual time scales, leading to large uncertainties in predictions of regional climate and ice cover.

Bai et al. (2012) conducted a systematic review of literature on Great Lakes climate and ice cover. Through thorough data analyses, they revealed several important findings: 1) Great Lakes ice cover and NAO have a linear relationship, 2) Great Lakes ice cover and Niño3.4 have a quadratic relationship, and 3) both Niño3.4 and NAO have competing impacts on lake ice cover; however, neither of them dominates. Based on these findings, a regression model was established to hindcast the lake ice cover using only NAO and Niño3.4 indices with a correlation of 0.56. Using this regression model, some extreme (both mild and severe) ice covers were underestimated. The model projected less ice for severe winters and more ice for the extreme mild winters. Although this model has been used since 2012 in early winter (between late December to early January) to predict annual maximum ice coverage (AMIC) each year using the projected NAO and Niño3.4 indices, it is often seen that the predicted AMIC is systematically lower than the observed AMIC in the severe winters. This indicates that some important predictive factors are missing.

With the last five years of data added to the ice dataset (Wang et al. 2012b), particularly with high ice cover during the last two winters, a timely update of the data is necessary for better understanding of mechanisms of decadal and multidecadal variability in lake ice (Magnuson et al. 2000; Ghanbari et al. 2009; Weyhenmeyer et al. 2011; Mishra et al. 2011). The purpose of this study is to establish updated regression models for better seasonal hindcast and projection of lake ice cover by using projected indices of teleconnection patterns.

2. Data

The lake ice coverage used in this study is from the Great Lakes Ice Atlas, updated from 1973-2015, based on the previous ice atlas (Wang et al. 2012b; http://www.glerl.noaa.gov/data/pgs/glice/glice.html). Wang et al. (2012b) have described the data sources, processing procedure, and quality control in great detail.

The Niño3.4 SST (Sea Surface Temperature) anomaly index was used as a marker of ENSO variability to identify the warm and cold episodes during 1973-2015 based on a threshold of +/- 0.5^{o}C. Cold and warm episodes are defined as those periods for which the threshold is met for a minimum of five consecutive over-lapping seasons such as November-December-January (NDJ), December-January-February (DJF), January-February-March (JFM), etc. Otherwise, the winter is defined as ENSO-neutral. The index is defined as the 3-month running mean of ERSST.v3 (Extended Reconstructed Sea Surface Temperature Version 3) SST anomalies in the Niño3.4 region (5^{o}N-5^{o}S, 120^{o}-170^{o}W; obtained from NOAA/CPC (Climate Prediction Center) http://www.cpc.noaa.gov/products/analysis_monitoring/_ensostuff/ensoyears.shtml). The strong warm (cold) winters are defined as the DJF periods when the mean index exceeds 1.0 (-1.0) °C, and weak warm (cold) winters are defined as the DJF periods when the mean index is greater than 0.5 (-0.5) °C, but less than 1.0 (-1.0) °C.

The monthly NAO index from 1973 to 2015 was obtained from the Climatic Research Unit, UK (http://www.cru.uea.ac.uk/cru/data/NAO.htm). The NAO is defined as the normalized pressure difference between a station on the Azores and one on Iceland. A winter is defined as having a positive (negative) phase when the DJF mean index exceeds +0.5 (-0.5) standard deviation, otherwise a winter is defined as NAO-neutral.

The Pacific Decadal Oscillation (PDO) index is the leading empirical orthogonal function (EOF) of monthly sea surface temperature anomalies (SSTA) over the North Pacific (poleward of 20° N) after the global mean SST has been removed. The PDO index is the standardized principal component time series (Mantua et al. 1997; Zhang et al. 1997) (http://research.jisao.washington.edu/pdo/PDO.latest; https://www.ncdc.noaa.gov/teleconnections/pdo/).

The Atlantic Multidecadal Oscillation (AMO) was identified by Schlesinger and Ramankutty (1994). The AMO signal is usually defined from the patterns of SST variability in the North Atlantic once any linear trend has been removed. This detrending is intended to remove the influence of greenhouse gas-induced global warming from the analysis. The AMO index is obtained from http://www.esrl.noaa.gov/psd/data/timeseries/AMO/.

3. Results

3.1 Annual maximum ice concentration 1973-2015

Great Lakes ice cover has been declining since 1973 (Wang et al. 2012a). With the last five years of data added to the Great Lakes Environmental Research Laboratory (GLERL) ice cover data base (Fig. 1), the time series of AMIC has a downward trend for all five individual lakes, and the entire basin, similar to the period 1973-2010 (Wang et al. 2012a). The linear trend was estimated using the least squares regression. The linear equation is in the form: x=a+bt, where x is the ice concentration, t is the year, a is the x-intercept constant (the value of x for t=1973), and b is the slope of the line (namely, the rate of change in x with a time increment of t).

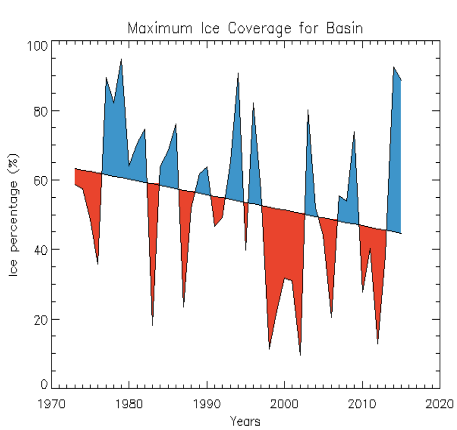

Figure 1. AMIC (in %) of the entire 5-Great Lakes for the period 1973-2015. The linear line is the trend in AMIC calculated from the least square fit method. Units for the vertical axes are in %.

3.2 Decadal variability

With the last five years (2011-2015) of data added to the previous time series (Wang et al. 2012a), the interannual variability further stands out, as does the decadal variability (Fig. 2). The decadal variability in small lakes was investigated by previous studies (Magnuson et al. 2000; Ghanbari et al. 2009; Weyhenmeyer et al. 2011). During this 43-year period, three high ice bands stand out: 1977-79, 1994, and 2014-15, with separation periods of 17 years and 21 years, respectively. Similarly, three low ice bands also stand out: 1983, 1998-2002, and 2010-2013, separated by around 18 and 12 years, respectively. The longest low ice band started in 1998 and lasted to 2013. The 1997/98 El Niño was the largest El Niño event of the century (Van Cleave et al. 2014), which caused a regime shift in lake ice cover and other environmental components.

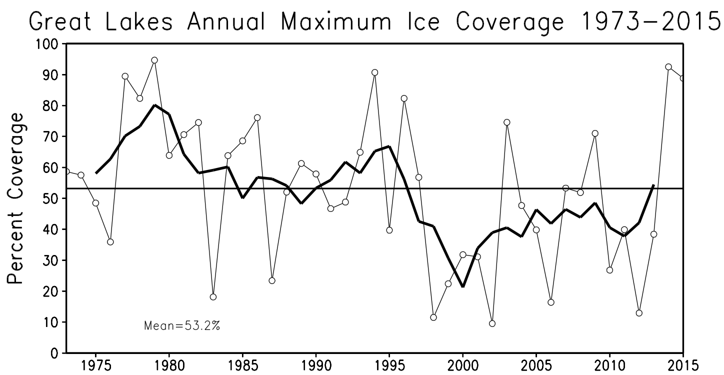

Figure 2. Time series of AMIC during 1973-2015. The thick line is the 5-year running mean, indicating the decadal signal.

4. Development of hindcast regression models

Based on the investigation above, multi-variable regression models can be constructed following Bai et al. (2012). The following model is the same as Bai et al. (2012) except that the data are extended to 2015, and it only includes NAO, Niño3.4, and their interaction:

$$Y=0.45 -0.016\text{Niño34} -0.5(\text{Niño3.4})^2 -0.42\text{NAO}+ 0.29\text{NAO}\bullet(\text{Niño3.4})^2 \quad (1)$$

where Y is normalized AMIC. The correlation between the model hindcast time series and the observed AMIC is R=0.44 (R^2=0.2) (see Fig. 3, blue).

When the AMO index is added to eq. (1), the correlation between the model and observation increases to R= 0.62 (R^2=0.38; see Fig. 3a, red) from the original 0.44 (figure not shown). The total variance increases to 38% from the original 20% by just adding AMO.

When the PDO index is added to eq. (1), the correlation also improves (R=0.56; not shown), compared to eq. (1), indicating that adding a linear impact of PDO improves the prediction skill, although not as high as AMO.

When both PDO and AMO are added to eq. (1), the correlation increases to R=0.64 (R^2=0.41), improving the hindcast skill compared to the individual contribution by the AMO (0.62) or the PDO (0.56).

As discussed above, the interaction or competing mechanisms of the teleconnection patterns on ice cover should be considered. These competing mechanisms include: 1) the NAO and Niño3.4 on interannual time scales, as discussed in Bai et al. (2012), 2) the NAO and AMO, Niño3.4 and PDO on crossing interannual and decadal time scales, and 3) the AMO and PDO on decadal time scales. Thus, the following comprehensive regression model is constructed:

$$\begin{aligned} Y=0.45 &-0.13\text{Niño3.4} -0.4(\text{Niño3.4})^2 -0.4\text{NAO}+ 0.21\text{NAO}\bullet(\text{Niño3.4})^2 \\ &-0.5\text{AMO}+0.15\text{PDO}+0.05\text{PDO}^2 \\ &+0.01\text{AMO}\bullet\text{NAO}-0.08\text{PDO}^2\bullet(\text{Niño3.4})^2 \\ &+0.16\text{PDO}^2\bullet\text{AMO} \end{aligned} \qquad (2)$$

The correlation further increases to R=0.684 (R^2=0.47). Therefore, including AMO and PDO and their interactions significantly improves the prediction skill (R=0.68) (Fig. 3, red) from the original model that only includes NAO and Niño3.4 (R=0.44; Fig. 3, blue).

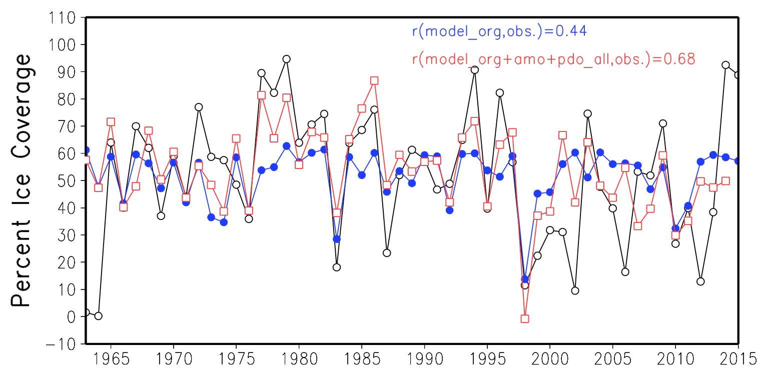

Figure 3. Original hindcast (Bai et al.,2012;blue), AMIC (black), and model with all the effects from NAO, AMO, Nino3.4, and PDO, and their combined competing mechanisms (red). The corresponding correlation between the model results and the observed AMIC are given.

5. Projection of Great Lakes AMIC during 2015/16 winter

The Great Lakes Climate Outlook required lake ice cover projection in the middle of the winter in 2016. On November 30, 2015, we collected available projected indices of Niño3.4, NAO, PDO, and AMO during December-January-February. It came out with Niño3.4=2.0, NAO=1.2, AMO=0.342, and PDO=0.5. Using model 1 (original using only NAO and Niño3.4 indices) and model 2 (new model using all four indices), AMIC in winter of 2015/16 was projected to be 38% and 31%, respectively, indicating model 2 produces lower extreme value than model 1. Figure 4 shows the observed ice cover on December 22, 2015 (left), which is nearly ice free, because the 2015/16 winter experiences so far the simultaneous strong El Niño and +NAO year. The observation showed that the AMIC on the Great Lakes was 34% on February 14, 2016 (Fig. 4, right), which was very close to the projection on November 30, 2015, with the relative error being less than 10%.

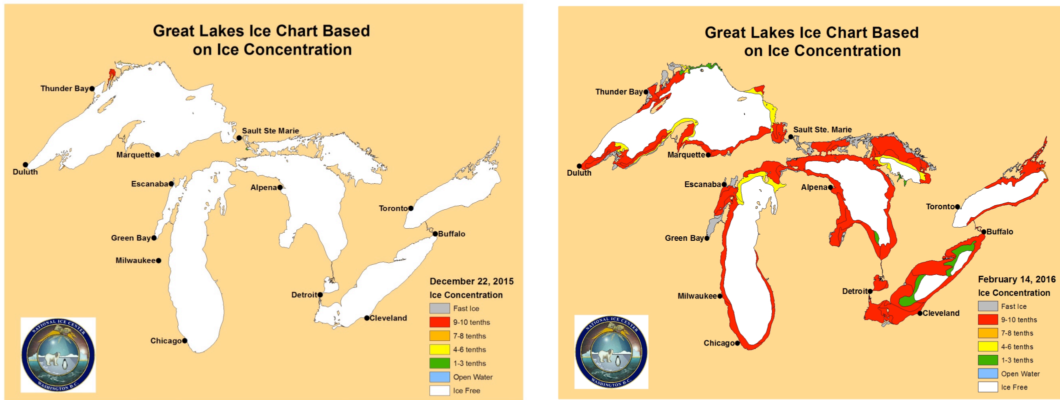

Figure 4. Satellite measured ice concentration in the Great Lakes on December 22, 2015 (left) and on February 14, 2016 (right, 34% coverage).

During the simultaneous El Niño and +NAO winter, surface air temperature experienced the warmest anomaly over the Great Lakes region (Fig. 5a), compared with the other combinations. Generally speaking, El Niño (La Niña) would produce warm (cold) anomalies, while positive (negative) NAO would produce warm (cold) anomalies, However, the competing effect of both forcings depends on their strength at the case-by-case manner.

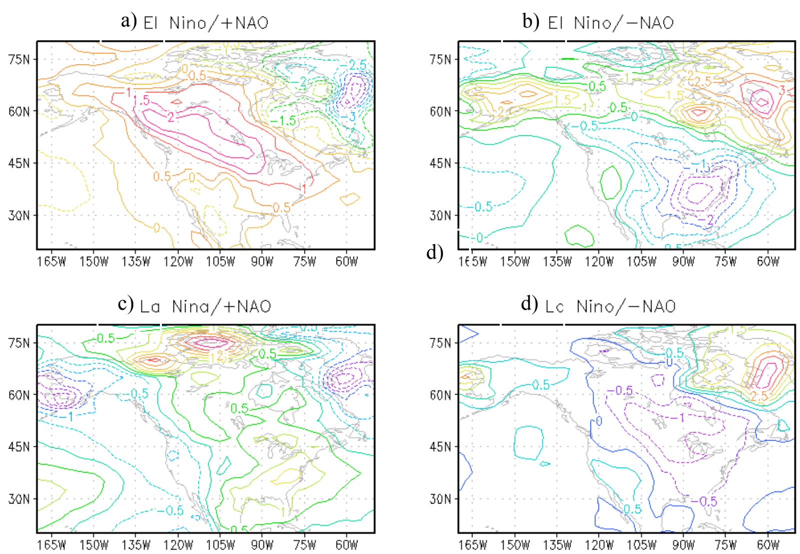

Figure 5. Composite maps of surface air temperature anomalies in North America for winters during (a) El Niño&+NAO; (b) El Niño&-NAO; (c) La Niña&+NAO; and (d) La Niña&-NAO. The intervals of SAT anomalies are 0.5°C, and dashed lines denote negative anomalies.

6. Conclusions

On the basis of the above investigation, the following conclusions can be drawn:

1) With the last five years of data (2011-2015) added to the analysis, in addition to large variability on interannual time scales, decadal variability in Great Lakes ice cover stands out. Lake ice downward trend reduced for the period 1973-2015, compared to the period 1973-2010.
2) Statistic regression hindcast models were tested using all four teleconnection patterns: NAO and Niño3.4 on interannual time scales, and AMO and PDO on decadal time scales.

The best model constructed here can capture 47% of the total variance of ice cover. The correlation coefficient between the hindcast model results and observations is 0.68. This model includes not only the interactions/competing effects within interannual time scales (NAO and Niño3.4) and within decadal time scales (AMO and PDO), but also includes the competing effects across interannual and decadal time scales such as within Niño3.4 and PDO, and within NAO and AMO.

3) The regression models were used to project AMIC in the 2015/16 winter, which was 31% using the new model, and 38% using the original model that include only Niño3.4 and NAO indices.

Acknowledgments. NCEP Reanalysis data was provided by the NOAA/OAR/ESRL PSD, Boulder, Colorado, USA, from their Web site at http://www.cdc.noaa.gov/. Support from U.S. EPA's Great Lakes Restoration Initiative (GLRI) to climate change and modeling studies is appreciated. We appreciate Nicole Rice for her editorial assistance. This is GLERL Contribution No. xxxx.

References

Bai, X. and J. Wang, 2012. Atmospheric teleconnection patterns associated with severe and mild ice cover on the Great Lakes, 1963-2011. *Water Quality Research Journal of Canada,* 43, 421-435.

Bai, X., J. Wang, C. Sellinger, A. Clites, and R. Assel, 2012. Interannual variability of Great Lakes ice cover and its relationship to NAO and ENSO. *J. Geophys. Res.,* doi:10.1029/2010JC006932.

Ghanbari, R.N., H.R. Bravo, J.J. Magnuson, W.G. Hyzer, B.J. Benson, 2009. Coherence between lake ice cover, local climate and teleconnections (Lake Mendota, Wisconsin). *J. Hydrol.,* 374, 282–293.

Magnuson, J.J, et al., 2000. Historical Trends in Lake and River Ice Cover in the Northern Hemisphere, *Science*, 289, 1743-1746.

Mantua, N.J. and S.R. Hare, Y. Zhang, J.M. Wallace, and R.C. Francis, 1997. A Pacific interdecadal climate oscillation with impacts on salmon production. *Bulletin of the American Meteorological Society*, 78, pp. 1069-1079.

Mishra, V, K.A. Cherkauer, L.C. Bowling, and M. Huber, 2011. Lake Ice phenology of small lakes: Impacts of climate variability in the Great Lakes region. *Global and Planetary Change*, 76: 166-185.

Schlesinger, M. E. and N. Ramankutty (1994). An oscillation in the global climate system of period 65-70 years. *Nature,* 367 (6465): 723–726.

Van Cleave, K., J. Lenters, J. Wang, and E. Verhamme, 2014. A regime shift in Lake Superior ice cover, evaporation, and water temperature following the warm El Niño winter of 1997-98. *Limnology and Oceanography* 59(6):1889-1898 (DOI:10.4319/lo.2014.59.6.1889).

Wang, J., X. Bai, G. Leshkevich, M. Colton, A. Clites, and B. Lofgren, 2010. Severe Great Lakes ice cover in winter 2008/09: Contribution of AO and ENSO, AGU *EOS, 91 (5), 41-42*.

Wang, J., X. Bai, H. Hu, A. Clites, M. Colton, and B. Lofgren, 2012a. Temporal and spatial variability of Great Lakes ice cover, 1973-2010. *J. Climate,* DOI: 10.1175/2011JCL14066.1

Wang, J., R.A. Assel, S. Walterscheid, A. Clites, and X. Bai, 2012b. Great Lakes ice climatology update: Winter 2006–2011 description of the digital ice cover data set, NOAA Technical Memorandum GLERL-155, 37 pp. 2012.

Weyhenmeyer, G.A., D.M.Livingstone, M. Meili, O. Jensen, B.J. Benson, and J.J. Magnuson. 2011. Large geographical differences in the sensitivity of ice-covered lakes and rivers in the Northern Hemisphere to temperature changes. *Global Change Biology* 17: 268-275.

Zhang, Y., J.M. Wallace, D.S. Battisti, 1997. ENSO-like interdecadal variability: 1900-93. *J. Climate*, 10, 1004-1020.